



HAL
open science

Electromechanical Properties of Piezoelectric Integrated Structures on Porous Substrates

Pierre Marechal, Franck Levassort, Janez Holc, Danjela Kuscer, Maria Kosec, Guy Feuillard, Marc Lethiecq

► **To cite this version:**

Pierre Marechal, Franck Levassort, Janez Holc, Danjela Kuscer, Maria Kosec, et al.. Electromechanical Properties of Piezoelectric Integrated Structures on Porous Substrates. *Ferroelectrics*, 2008, 371 (1), pp.89 - 97. 10.1080/00150190802396850 . hal-03840978

HAL Id: hal-03840978

<https://hal.science/hal-03840978>

Submitted on 16 Jan 2023

HAL is a multi-disciplinary open access archive for the deposit and dissemination of scientific research documents, whether they are published or not. The documents may come from teaching and research institutions in France or abroad, or from public or private research centers.

L'archive ouverte pluridisciplinaire **HAL**, est destinée au dépôt et à la diffusion de documents scientifiques de niveau recherche, publiés ou non, émanant des établissements d'enseignement et de recherche français ou étrangers, des laboratoires publics ou privés.

Electromechanical properties of piezoelectric integrated structures on porous substrates

P. MARECHAL,¹ F. LEVASSORT,¹ J. HOLC,² D. KUŠČER,²
M. KOSEC,² G. FEUILLARD,¹ AND M. LETHIECQ^{1,*}

¹François-Rabelais University, LUSI, FRE 2448 CNRS, ENIVL, rue de la
Chocolaterie, 41000 Blois, France

²Joseph Stefan Institute, Jamova 39, Ljubljana, Slovenija

The fabrication of piezoelectric transducers for high resolution medical imaging applications requires a backing material to damp the piezoelectric resonance, resulting in a shorter time response, i.e. improved resolution, but lower sensitivity. Thus, the choice of such a substrate must be made according to its acoustical properties, namely the ratio of acoustical impedance of the backing material and the piezoelectric layer. Moreover, this backing material must have a relatively high attenuation, and provide good surface properties such as a low roughness and diffusion potential. Finally, the substrate material must have a good mechanical behavior at high temperature (around 900°C for the sintering of the piezoelectric thick film). In this context a review of available materials is first given, and the corresponding list is found to be quite limited. Several PZT/PGO piezoelectric thick films deposited by screen-printing have been fabricated on dense alumina [1] and have delivered good electromechanical performance, but the substrate attenuation was too low to be used as a backing for high frequency transducers. In this paper, new porous Al₂O₃ substrates have been fabricated and used for the fabrication of a batch of piezoelectric films. The effects of a barrier layer and bottom electrode (conductive material type and thickness) are studied and related to the electromechanical performance of the piezoelectric thick film and then to the electro-acoustic properties of the ultrasonic transducer integrating these structures. Finally, these results are compared with previous studies [2] using porous PZT substrate. These comparisons are performed in terms of fabrication facility, electromechanical constants of the thick films (in thickness mode) and electro-acoustic responses of ultrasonic transducers with center frequencies over 20 MHz.).

Keywords Integrated structures; piezoelectric transducer; high frequency

A. Introduction

The elaboration of piezoelectric ultrasonic transducers with integrated thick film structures [1–3] necessitates a substrate that withstands the sintering temperature. Moreover, the substrate properties must be compatible with those of the screen-printed layers in terms of thermal and mechanical properties, chemical neutrality, acoustic impedance and attenuation. This substrate is to be chosen among available materials, *i.e.* pure materials (Si, Al, ...) metal oxides (SiO₂, ZrO₂, PZT, Al₂O₃, ...), compatible with this fabrication process. In

this study, two possible candidates were characterized and compared: PZT and Al_2O_3 . Nevertheless, such substrates still have a high acoustic impedance leading to a strong damping of the piezoelectric resonance [2]. Their acoustic impedance can be lowered by the addition of pore formers during their sintering. During the fabrication of the substrate, the addition of pore formers allows the porosity level to be increased, consequently decreasing the acoustic impedance and increasing the attenuation. The acoustic impedance ratio of the substrate and piezoelectric layer is first considered, as it is a key parameter of the piezoelectric resonance damping, allowing to tailor the bandwidth of the transducer. The fabrication process of porous substrates is briefly described. Secondly, the characterization results of these porous substrates is discussed both for PZT and Al_2O_3 , in comparison with dense substrates. Thirdly, ultrasonic transducers are manufactured with both chosen substrates. The influence of the acoustic impedances is discussed both in terms of sensitivity and relative bandwidth of the transducer. Then, the influence of the layers placed between the thick film and its substrate on the input (effective) acoustical impedance of the backing is discussed. Finally, experimental results are compared for integrated transducers based on porous PZT and porous Al_2O_3 substrate.

B. Fabrication

The fabrication of an integrated thick film structure is presented, from the porous substrate to the screen-printing of the piezoelectric layer. This substrate which has to withstand the sintering temperature is fabricated to fulfill the transducer backing acoustical specifications. Here two candidates are compared: porous PZT and porous Al_2O_3 .

B.1. Substrate

The requirements for a substrate are its ability to withstand the sintering temperature of the piezoelectric thick film, its mechanical properties and its chemical neutrality. To be used as a backing, the substrate must have a relatively low acoustic impedance compared to that of the future piezoelectric layer. Its attenuation must also be high enough to avoid echoes from its rear face. Previous studies had identified porous PZT substrate as a satisfactory candidate [4]. PZT powder was synthesized by mixed oxide synthesis with double calcination at 900°C . Then, it was mixed with ammonium oxalate to increase porosity. Finally, its microstructure was analyzed and characterized (Fig. 1(a)). The volume fraction of porosity was measured at $v_f = 14\%$. Here, this reference porous PZT substrate is compared with a porous Al_2O_3 substrate, fabricated from fine (Alcoa A 16) and coarse (Alcoa CL 3000) alumina powder in equal mass ratio. After homogenization in ball mill, the powder was pressed into

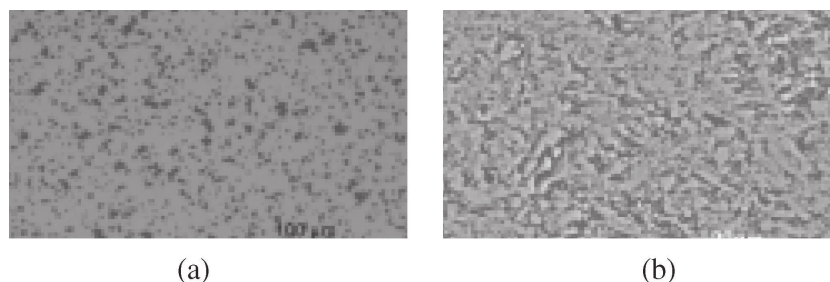


Figure 1. Microstructure of (a) porous PZT and (b) porous Al_2O_3 .

Table 1
Acoustic properties of porous substrates

Substrate	v_f (%)	ρ (kg/m ³)	c_l (m/s)	Z (MRa)	α (dB/mm/MHz)
Porous PZT	14	6660	2730	18.2	0.26
Porous Al ₂ O ₃	23	3250	5900	17.7	0.15

v_f : volume fraction of porosity; ρ : density; c_l : longitudinal wave velocity; Z : acoustic impedance; α : attenuation.

pellets and sintered at 1450°C. Based on a micro-structure analysis (Fig. 1 (b)), the volume fraction of porosity was evaluated around $v_f = 23\%$.

On the basis of these evaluations of the porosity level, an homogenization model with 3-0 connectivity was used in order to deduce the effective acoustic properties of the substrates (Table 1). Transmission measurements were performed to adjust the properties and to estimate the attenuation of the substrates.

B.2. Screen-Printing

Based on previous studies, a diffusion of the rear electrode into the substrate was observed during thick film sintering. Therefore, a barrier layer is first screen-printed in order to avoid this phenomena in both substrates. The screen-printing process was adjusted depending on the compatibility problems encountered between the functional layers. On the porous PZT substrate (Fig. 2(a)), a barrier layer of PZT/PGO paste is screen-printed in two passes and

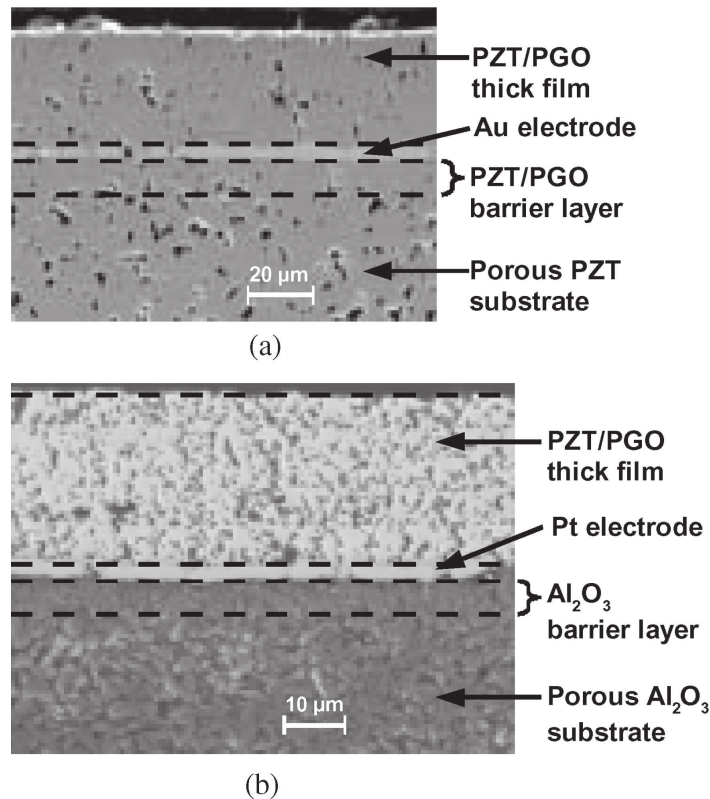


Figure 2. SEM cross-section photograph of an integrated structure on (a) porous PZT and (b) porous Al₂O₃ substrates.

sintered at 900°C. A gold paste is screen-printed in one pass to constitute the rear electrode. Then, a PZT/PGO paste is screen-printed in six passes with an intermediate sintering stage in order to avoid cracks in the future piezoelectric layer. Following sintering, a gold electrode is sputtered at the top. This integrated structure is then poled in a oil bath at 150°C for 15 min, under an electrical field of 12 kV/mm. On the porous Al₂O₃ substrate (Fig. 2 (b)), the barrier layer is made of two passes of fine alumina powder (Alcoa A 16) paste and sintered at 1400°C for 2 h. The bottom platinum electrode is formed from a paste (Ferro 6412-0410), printed twice and sintered at 1200°C for 2 h. Then, a PZT/PGO paste is printed in five passes and sintered at 800°C for 8 h under saturated PbO atmosphere in order to increase its density. Finally, a gold electrode is sputtered at the top. The piezoelectric layer is then poled in a oil bath at 160°C for 5 min, under an electrical field of 3 kV/mm. SEM cross sections (Fig. 2) allow to evaluate the thicknesses of the constitutive layers. Due to the porosity level, the diffusion phenomena can still have a strong influence on thicknesses variations ($\pm 5 \mu\text{m}$), leading to local discontinuities for thin layers.

C. Characterisation Results

On the basis of a preliminary thickness evaluation of the constitutive layers, the electromechanical parameters of the thickness mode can be identified.

C.1. Thickness and Acoustic Properties

The mean thickness t and the volume fraction of porosity v_f were measured in each constitutive layer, and density ρ was calculated. Then, the longitudinal wave velocity c_l and acoustic impedance Z can be deduced (Table 2). The density of the substrate was previously determined, as well as its longitudinal wave velocity. For the integrated structure based on a porous PZT substrate, a density $\rho = 6900 \text{ kg/m}^3$ was deduced for the PZT/PGO barrier layer and piezoelectric thick film. Their longitudinal wave velocity was deduced at $c_l = 3500 \text{ m/s}$ or $c_l = 4300 \text{ m/s}$, when considering either unpoled or poled PZT/PGO, for the PZT/PGO barrier layer and piezoelectric thick film, respectively. Similarly for the porous Al₂O₃ substrate, the density of the piezoelectric thick film was evaluated at $\rho = 7000 \text{ kg/m}^3$ and the longitudinal wave velocity at $c_l = 4170 \text{ m/s}$. The density of the Al₂O₃ barrier layer was evaluated at $\rho = 3600 \text{ kg/m}^3$ and the corresponding longitudinal wave velocity was found to be $c_l = 6500 \text{ m/s}$. Since the electrodes were considered to be pure metals, either gold or platinum, their acoustical properties were imposed.

Table 2
Layer properties of the integrated structures

Substrate Property	Porous PZT		Porous Al ₂ O ₃	
	Z (MRa)	t (μm)	Z (MRa)	t (μm)
Front electrode	63.8	0.5	63.8	0.1
Thick film	29.8	32	29.2	33
Back electrode	63.8	5	84.7	8
Barrier layer	24.0	12	23.4	10
Substrate	18.2	10000	19.2	12000

Z: acoustic impedance; t : thickness.

Table 3
Electromechanical properties of the piezoelectric thick film

Substrate	Z (MRa)	ρ (kg/m ³)	c_l (m/s)	k_t (%)	$\frac{\epsilon_{33}^s}{\epsilon_0}$	δ_m (%)	δ_e (%)
Porous PZT	29.8	6900	4300	41	510	22	0.5
Porous Al ₂ O ₃	29.2	7000	4170	41	680	12	1.0

Z: acoustic impedance; ρ : density; c_l : longitudinal wave velocity; k_t : thickness coupling coefficient; $\epsilon_{33}^s/\epsilon_0$: relative dielectric constant; δ_m , δ_e : mechanical, dielectric losses.

C.2. Electromechanical Properties

The electrical impedance $Z_e(f)$ was measured around the fundamental thickness mode resonance of the integrated structure. The KLM model was used to simulate and fit the electrical impedance $Z_e(f)$ of this integrated structure constituted of a substrate, a barrier layer, a back electrode, a piezoelectric thick film and a front electrode. The missing electromechanical properties of the piezoelectric thick film were fitted (Table 3) and compared for both integrated structures based on porous PZT or porous Al₂O₃ substrates.

Measurements and corresponding fits are represented for these two integrated structures (Fig. 3). The first thickness mode of the piezoelectric layer is characterized by the anti-resonance frequency of the free piezoelectric thick film $f_a = c_l/(2t_p)$, where c_l is the longitudinal wave velocity and t_p is the thickness of the piezoelectric thick film. It results in $f_a = 67$ and 63 MHz for the PZT and Al₂O₃ substrates respectively. Nevertheless, one can observe that the anti-resonance peak of the integrated structure $f_0 = 42$ and 40 MHz is lowered and widened in comparison with that of a free piezoelectric disk f_a . This phenomenon is well known as a result of the load of the backing. Here, the damping of the resonance is a result of the complex effective acoustic impedance load seen at the rear face of the piezoelectric layer, *i.e.* the acoustic impedance of the substrate seen through the barrier and rear electrode layers.

C.3. Acoustic Impedance Ratios

This damping effect can be quantified by the ratio of the effective acoustic impedance of the backing and of the active piezoelectric layer $|Z_{in,back}|/Z_p$. The closer to 1 this acoustic impedance ratio, the higher the damping. This results in a lower resonance frequency and lower sensitivity of the ultrasonic transducer. Based on the evaluated thicknesses and acoustic properties, the effective acoustic impedance of the backing can be calculated recursively from the substrate ($Z_{in,N+1} = Z_s$) to the rear face of the piezoelectric layer ($Z_{in,1} = Z_{in,back}$), where N is the number of finite length layers. Here, there are $N = 2$ layers between the piezoelectric layer and the substrate (considered as semi-infinite). The effective acoustic impedance of the backing $Z_{in,1} = Z_{in,back}$ is illustrated for both integrated structures based on porous PZT (Fig. 4(a)) or porous Al₂O₃ (Fig. 4(b)) substrates.

As it can be observed, the acoustic impedance ratio between the substrate and the piezoelectric layer is nearly the same for both structures: $Z_s/Z_p = 0.61$ and 0.66, for the porous PZT and Al₂O₃ substrates, respectively. Nevertheless, the barrier layer and rear electrode must be taken into account. The barrier layer has little effect, since its acoustic impedance is relatively similar to that of the substrate. The back electrode has a stronger effect, since its acoustic impedance is significantly different from those of the barrier layer and substrate, and its thickness is not negligible as compared to the wavelength. This results

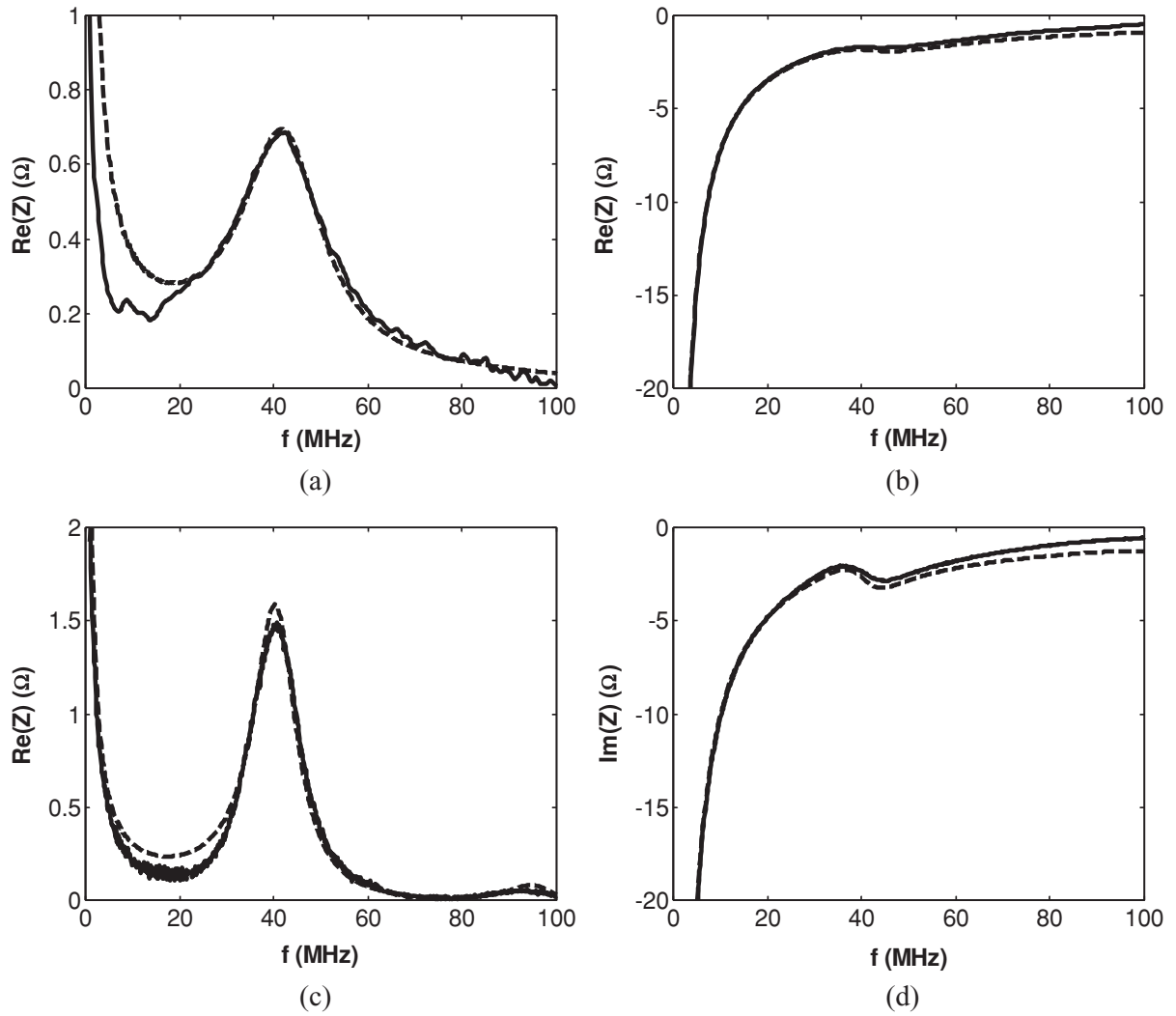


Figure 3. Experimental (solid) and modeled (dashed) (a), (c) real and (b), (d) imaginary parts of the electrical impedance $Z_e(f)$ of the integrated piezoelectric structure based on (a), (b) porous PZT and (c), (d) porous Al_2O_3 substrates.

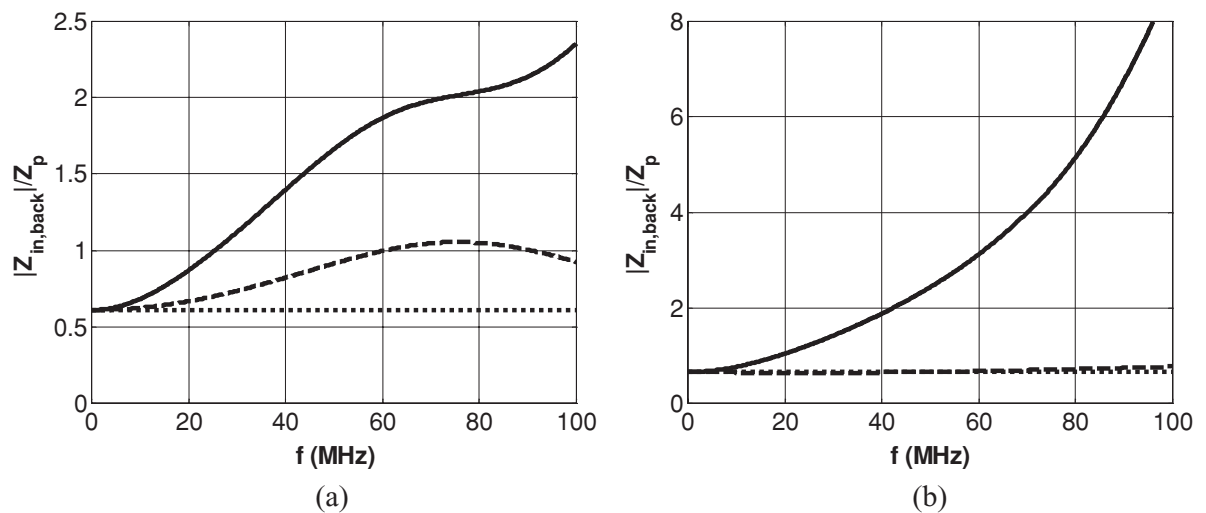


Figure 4. Modulus of the acoustic impedance ratio (to the thick film value) of the substrate (dotted), the barrier layer (dashed) and the backing (solid), for the integrated piezoelectric structure based on (a) porous PZT and (b) porous Al_2O_3 substrates.

in an effective impedance of the backing that varies as a function of frequency. Since the anti-resonance frequency of the integrated structure is around 40 MHz, the frequency range of interest is from 20 to 60 MHz. In this range, the acoustic impedance ratio $|Z_{\text{in,back}}|/Z_p$ increases nearly linearly from 0.9 to 1.9 for the integrated structures based on porous PZT substrate, whereas it varies from 1 to 3 for the integrated structures based on porous Al_2O_3 substrate.

D. Transducer Fabrication and Characterisation

After the screen-printing process, the transducer is fabricated: electrical contacts on back and front electrodes are performed to connect the transducer to a pulser/receiver via a coaxial cable. An isolating tube and a metallic housing are added and epoxy putting is used to maintain the assembly. Then, the pulse-echo electro-acoustic responses of the two integrated ultrasonic transducers were evaluated and discussed.

D.1. Electroacoustic Performance

The performance of the PZT porous substrate based transducer was first evaluated in water, with $Z_{\text{front}} = Z_{\text{water}} = 1.5 \text{ MRa}$ the data of which is summarized in Tables 1 to 3. At the rear face, the acoustic impedance ratio $|Z_{\text{in,back}}|/Z_p$ was previously estimated from 0.9 to 1.9 around the resonance frequency f_0 . It results in a short electro-acoustic response (Fig. 5(a)) and broad bandwidth (Fig. 5(b)), as is required for high resolution transducers. The theoretical KLM result is compared to measurements and found to be in good agreement (Fig. 5). The axial resolution normalized to the wavelength is evaluated at $\Delta z_6/\lambda_0 = 0.83$, and the relative bandwidth at -6 dB is estimated around $BW_{6,r} = 88 \%$. The main drawbacks of such a structure are its low electrical impedance (resulting in poor electrical matching to typical 50 ohm cables electronics) and low sensitivity.

D.2. Lens-Focused Transducer Electroacoustic Properties

To be used in applications such as high resolution medical imaging, a suitable trade-off between lateral resolution and depth of field of the transducer must be imposed with the addition of a focusing lens on its front face. In a previous study [5], it was demonstrated that

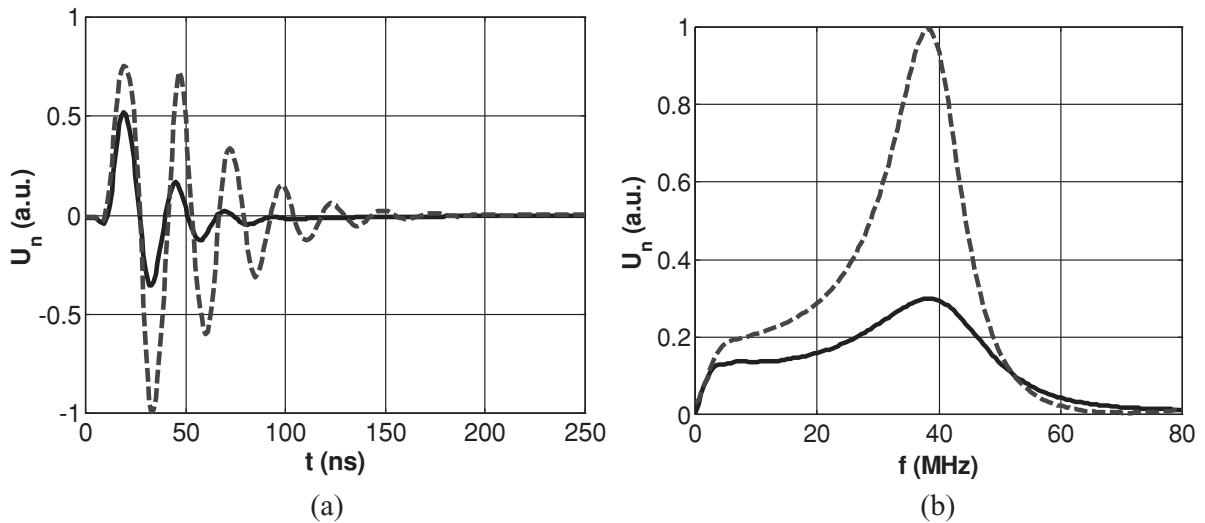


Figure 5. Experimental (solid) and modeled (dashed) normalized pulse-echo (a) electro-acoustic response and (b) frequency spectrum obtained for the integrated transducer based on a porous PZT substrate immersed in water.

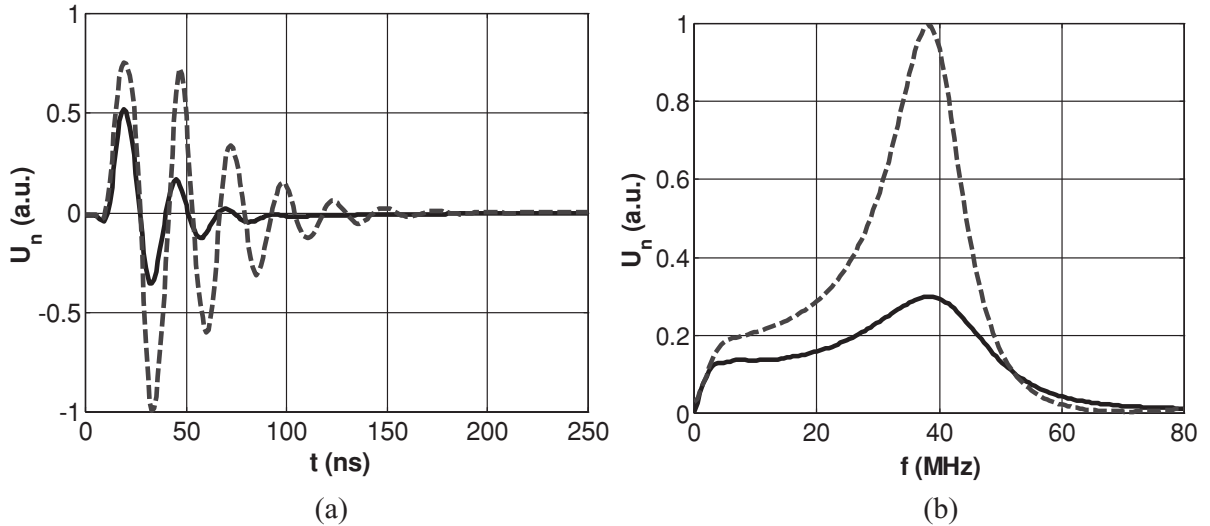


Figure 6. Normalized pulse-echo (a) electro-acoustic response and (b) frequency spectrum obtained in water with a focusing lens on the front face, for the integrated transducer based on a porous PZT (solid) and porous Al_2O_3 (dashed) substrates.

the focusing lens is seen as a semi-infinite medium by the integrated structure. Thus, the result $Z_{\text{front}} \approx Z_{\text{lens}} = 3 \text{ MRA}$ and data summarized in Tables 1 to 3 were used to simulate the pulse-echo electro-acoustic response of both integrated structures based on porous PZT and porous Al_2O_3 substrates using the KLM model (Fig. 6). The performance can therefore be compared for a realistic transducer configuration: the normalized axial resolution to the wavelength is evaluated at $\Delta z_6/\lambda_0 = 0.83$ and 1.58 and the relative bandwidth is estimated around $BW_{6,r} = 88\%$ and 43% , for the integrated structure based on porous PZT and porous Al_2O_3 substrates, respectively. In such operating conditions, the sensitivity would be 10 dB lower for the PZT substrate transducer relatively to that of the Al_2O_3 substrate device. Thus a trade-off is to be made between high axial resolution with low sensitivity (PZT), and high sensitivity with low axial resolution (Al_2O_3).

E. Conclusion

Two porous materials have been tested as a substrate for an integrated screen-printed piezoelectric structure designed to be used as ultrasonic transducer for high resolution medical imaging. Namely, porous PZT and porous Al_2O_3 were investigated as possible candidates to fulfill the function of transducer backing at the same time as that of substrate for the deposit of the piezoelectric thick film. The fabrication process and relevant chemical and mechanical requirements have been described. The role of the material properties and porosity level was highlighted, not only for the substrate, but also for the layers at the rear face of the piezoelectric thick film. Particularly, the thickness of the back electrode was shown to strongly modify the effective acoustic impedance of the backing and the related transducer electro-acoustic response. Finally, characterization results were obtained and discussed. For both substrates, axial resolution and bandwidth were deduced, as well as sensitivity, and it was shown that the two devices correspond to distinct performance trade-offs, both of which are compatible with medical diagnosis applications: very high resolution imaging at limited distance range for the PZT substrate device, imaging at larger distance range or Doppler blood flow measurements for the Al_2O_3 substrate device. The study has also shown

that a precise control and optimization of the back electrode thickness and properties are an essential design parameter.

Acknowledgments

This work was supported by the EC through the MINUET project (6th Framework Program, Contract No. NMP2-CT-2004-505657) and through the Network of Excellence MIND.

References

1. M. Kosec, J. Holc, F. Levassort, L. P. Tran-Huu-Hue, and M. Lethiecq, Screen-printed Pb(Zr,Ti)O₃ thick films for ultrasonic medical imaging applications invited talk at IMAPS 2001, Proceedings of the 34th International Symposium on Microelectronics, pp. 195–200, Baltimore, 9–11 October 2001.
2. P. Marechal, F. Levassort, J. Holc, L. P. Tran-Huu-Hue, M. Kosec, and M. Lethiecq, High frequency transducers based on integrated piezoelectric thick films for medical imaging. *IEEE TUFFC*, **53**, 1524–1533 (2006).
3. Kui Yao, Xujiang He, Yuan Xu, and Meima Chen, Screen-printed piezoelectric ceramic thick films with sintering additives introduced through a liquid-phase approach. *Sensors and Actuators A: Physical*, **118-2**, 342–348 (2005).
4. J. Holc, F. Levassort, P. Marechal, L. P. Tran-Huu-Hue, and M. Kosec, Screen-printed PZT thick film on porous PZT substrate, Processing of Electroceramics, Bled, Slovenia, 31 August-3 September (2003).
5. P. Marechal, F. Levassort, L. P. Tran-Huu-Hue, and M. Lethiecq, Lens-focused transducer modeling using an extended KLM model. *Ultrasonics*, 2007, to be published.